J|A|C|S
ARTICLES
Published on Web 07/07/2007

Depth Profiling of Water Molecules at the Liquid−Liquid Interface Using a Combined Surface Vibrational Spectroscopy and Molecular Dynamics Approach

Dave S. Walker and Geraldine L. Richmond*

Contribution from the Department of Chemistry and Materials Science Institute, University of Oregon, Eugene, Oregon 97403

Received March 21, 2007; E-mail: Richmond@uoregon.edu

Abstract: The studies presented here combine experimental and computational approaches to provide new insights into how water structures and penetrates into the organic phase at two different liquid−liquid systems: the interfaces of carbon tetrachloride−water (CCl_4-H_2O) and 1,2-dichloroethane−water (DCE−H_2O). In particular, molecular dynamics simulations are performed to generate computational spectral intensities of the CCl_4-H_2O and DCE−H_2O interfaces that are directly comparable with experimental measurements. These simulations are then applied toward the generation of spectral *profiles*, responses that vary as functions of both frequency and interfacial depth. These studies emphasize the similarities and differences in the structure, orientation, and bonding of interfacial water as a function of interfacial depth for these two liquid−liquid systems and demonstrate the differing behavior of water monomers that penetrate into the organic phase.

Introduction

There has been a growing interest in the molecular structure of the interface between two immiscible liquids. This is driven in part by the unique properties of the liquid−liquid interface for materials synthesis, its importance in understanding environmental remediation processes, and its relevance to understanding transport across biological membranes. These systems thus present an intriguing environment that is the focus of many applied and fundamental studies. From an applied perspective, they serve as the locale for processes such as chemical separations, nanoparticle synthesis, and charge transfer. From a fundamental perspective, they are amenable to experimental techniques such as X-ray reflectivity,[1−4] fluorescence anisotropy,[5] second harmonic generation (SHG) spectroscopy,[6−8] and vibrational sum frequency (VSF) spectroscopy.[9−16] Computational simulations of these liquid−liquid systems have also provided a great deal of insight, where properties such as interfacial width, molecular structure, dynamics, or spectroscopic response can be identified on a molecular scale.[17−28]

Of these experimental and computational techniques, VSF spectroscopy is proven to be a particularly powerful method for understanding the structure of the liquid−liquid interface.[9−16] However, while VSF spectroscopy has been applied to study a variety of liquid−liquid systems, use of the spectral results to obtain information regarding interfacial depth is very difficult. This is due to the fact that VSF spectroscopy is an excellent probe of the molecular bonding interactions extant within the interfacial region, yet the observed spectral response is also integrated over the entire interfacial region. X-ray reflectivity has been demonstrated to be a very good technique when applied toward the measurement of interfacial depth.[3] SHG spectroscopy has been used in conjunction with probe molecules of varying lengths, or so-called "molecular rulers", to sample interfacial properties at various depths.[7] But neither of these techniques

(1) Mitrinovic, D. M.; Zhang, Z.; Williams, S. M.; Huang, Z.; Schlossman, M. L. *J. Phys. Chem. B* **1999**, *103*, 1779.
(2) Tikhonov, A. M.; Mitrinovic, D. M.; Li, M.; Huang, Z.; Schlossman, M. L. *J. Phys. Chem. B* **2000**, *104*, 6336.
(3) Schlossman, M. L. *Curr. Opin. Colloid Interface Sci.* **2002**, *7*, 235.
(4) Luo, G.; Malkova, S.; Pingali, S. V.; Schultz, D. G.; Lin, B.; Meron, M.; Benjamin, I.; Vanysek, P.; Schlossman, M. L. *J. Phys. Chem. B* **2006**, *110*, 4527.
(5) Ishizaka, S.; Habuchi, S.; Kim, H.-B.; Kitamura, N. *Anal. Chem.* **1999**, *71*, 3382.
(6) Steel, W. H.; Walker, R. A. *Nature* **2003**, *424*, 296.
(7) Steel, W. H.; Lau, Y. Y.; Beildeck, C. L.; Walker, R. A. *J. Phys. Chem. B* **2004**, *108*, 13370.
(8) Wang, H.; Borguet, E.; Eisenthal, K. B. *J. Phys. Chem. B* **1998**, *102*, 4927.
(9) Richmond, G. L. *Chem. Rev.* **2002**, *102*, 2693.
(10) Scatena, L. F.; Richmond, G. L. *J. Phys. Chem. B* **2001**, *105*, 11240.
(11) Brown, M. G.; Walker, D. S.; Raymond, E. A.; Richmond, G. L. *J. Phys. Chem. B* **2003**, *107*, 237.
(12) Walker, D. S.; Brown, M. G.; McFearin, C. L.; Richmond, G. L. *J. Phys. Chem. B* **2004**, *108*, 2111.
(13) Gragson, D. E.; Richmond, G. L. *J. Phys. Chem. B* **1998**, *102*, 3847.
(14) Leich, M. A.; Richmond, G. L. *Faraday Discuss.* **2005**, *129*, 1.
(15) Knock, M. M.; Bell, G. R.; Hill, E. K.; Turner, H. J.; Bain, C. D. *J. Phys. Chem. B* **2003**, *107*, 10801.
(16) Du, Q.; Freysz, E.; Shen, Y. R. *Science* **1994**, *264*, 826.
(17) Benjamin, I. *J. Chem. Phys.* **1992**, *97*, 1432.
(18) Benjamin, I. *J. Phys. Chem. B* **2005**, *109*, 13711.
(19) Chang, T. M.; Dang, L. X. *J. Phys. Chem. B* **1997**, *101*, 10518.
(20) Dang, L. X. *J. Phys. Chem. B* **2001**, *105*, 804.
(21) Dominguez, H.; Berkowitz, M. L. *J. Phys. Chem. B* **2000**, *104*, 5302.
(22) Jedlovszky, P.; Vincze, A.; Horvai, G. *Phys. Chem. Chem. Phys.* **2004**, *6*, 1874.
(23) Madurga, S.; Vilaseca, E. *J. Phys. Chem. A* **2004**, *108*, 8439.
(24) Pratt, L.; Pohorille, A. *Chem. Rev.* **2002**, *102*, 2671.
(25) Senapati, S.; Berkowitz, M. L. *Phys. Rev. Lett.* **2001**, *87*, 176101.
(26) Hore, D. K.; Walker, D. S.; Richmond, G. L. *J. Am. Chem. Soc.* **2006**, *129*, 752.
(27) Hore, D. K.; Walker, D. S.; MacKinnon, L.; Richmond, G. L. *J. Phys. Chem. C* **2007**, *111*, 8832.
(28) Walker, D. S.; Moore, F. G.; Richmond, G. L. *J. Phys. Chem. C* **2007**, *111*, 6103.

 10.1021/ja071740b CCC: $37.00

can match the molecular-level bonding information that can be measured from vibrational spectroscopic methods.

In this work, molecular dynamics simulations are performed to generate VSF spectral intensities of water at the carbon tetrachloride−water (CCl_4−H_2O) and 1,2-dichloroethane−water (DCE−H_2O) interfaces. These computational measurements are found to be in very good agreement with experimental measurements. The simulations are then applied toward the generation of VSF spectral profiles. These spectral profiles are measured as functions of both frequency and interfacial depth, thus providing the molecular-level bonding information obtainable from VSF spectroscopic methods while elucidating this information as a function of location with respect to the interfacial region. Emphasis is placed upon the OH stretch modes of water that are immersed in the organic phases. These VSF profiles provide a unique description of interfacial depth that is difficult to determine from VSF spectral intensities typically measured in experiments.

Computational Details

Molecular dynamics simulations of the CCl_4−H_2O and DCE−H_2O interfaces were performed using the AMBER 7 package.[29] Details of the simulations have been described elsewhere,[28] so only a brief summary will be given here. Bulk liquid boxes measuring 40 Å × 40 Å × 40 Å were simulated for 200 ps. Each liquid box contained 2135 POL3 water molecules, 400 CCl_4 molecules, or 480 DCE molecules. Following equilibration of the bulk liquids, one water box was combined with one CCl_4 box to create a system measuring 40 Å × 40 Å × 80 Å, and one water box was combined with two DCE boxes to create a system measuring 40 Å × 40 Å × 120 Å. In both systems, statistics were only collected for the 40 Å × 40 Å × 80 Å volumes immediately surrounding the water region. This rendered the remaining DCE volume as a reservoir to accommodate the greater solubility of water in DCE with respect to CCl_4. These interfacial systems were minimized and simulated for 2 ns with periodic boundaries applied in all three directions. After this 2 ns equilibration, statistics were collected every 50 fs over the course of the next 3 ns. The time step of integration was 1 fs. The Particle Mesh Ewald technique applied an 8 Å cutoff to handle long-range interactions, and the temperature was held fixed at 300 K using weak coupling to a heat bath. A modified Morita and Hynes[30] treatment was applied to generate the VSF spectral responses from water within these liquid−liquid systems. These modifications included a dipole−dipole coupling term between adjacent water molecules and a variable intramolecular coupling constant for individual water molecules.[31] All spectra described in this report were determined for SSP polarization, which probes the transition dipole moments of OH stretch modes in water that oscillate perpendicular to the interface.

In the computational approach contained herein, emphasis was placed on revealing the VSF responses from the OH stretch modes of water that interact directly with the organic phase. Three types of interfacial water molecules possess OH stretch modes that fit into this category: water molecules that "straddled" the interface where one of the OH bonds (the "free OH" stretch mode) extended away from the water region; water molecules that were hydrogen bonded to other water molecules only on their oxygen atoms, labeled here as hydrogen bond acceptors; and water molecules that did not possess any hydrogen bonds, labeled here as water monomers. It should be noted that, computationally, any water molecule that possessed a hydrogen bond on *only one* of its two hydrogen atoms was characterized as a straddling water molecule; this was independent of (i) the number of hydrogen bonds on their oxygen atoms and (ii) the actual location of these molecules with respect to the interfacial region. These generalities were in accordance with the current identification of the free OH mode extracted from VSF experimental measurements.[10,28] Finally, the criterion for hydrogen bonding was an intermolecular O−H separation of 2.5 Å. (This value was generous, as the local minimum from the O−H radial distribution function for this water model in this configuration was determined to be approximately 2.4 Å.)

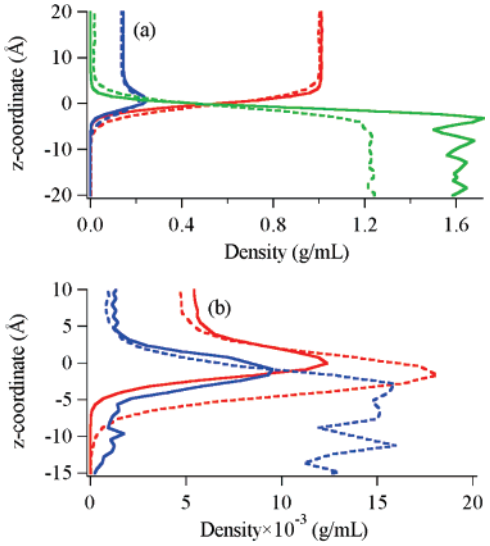

Figure 1. (a) Density profiles of water (red), straddling water molecules (blue), and organic liquids (green) at the CCl_4−H_2O (solid) and DCE−H_2O (dashed) interfaces. (b) Density profiles of hydrogen bond acceptors (red) and water monomers (blue) at the CCl_4−H_2O (solid) and DCE−H_2O (dashed) interfaces. Density profiles of water monomers have been scaled by 20× to fit the graph. Resolution (bin size) for each graph is 1 Å.

Results and Discussion

Figure 1a and 1b show density profiles of the CCl_4−H_2O (solid lines) and DCE−H_2O (dashed lines) systems as a function of interfacial depth along the *z*-coordinate of the periodic cell. The *z*-coordinate is represented here as the vertical axis and is normal to the interfacial plane. The density region above 0 Å represents the water phase, while the density region below 0 Å represents the organic phase. Figure 1a shows the density profiles of water, CCl_4, DCE, and water molecules that straddle the interface. Although straddling water molecules possess population within bulk water (above 0 Å), Figure 1a shows that their population peaks at the interface. The density profile of DCE approaches the interfacial region smoothly and extends slightly deeper into the bulk water phase when compared to that of CCl_4. This is indicative of the increased interfacial thickness of the DCE−H_2O interface compared to the that of the CCl_4−H_2O interface and is reported in other experimental and computational observations.[18,32] The density profile of CCl_4 however appears oscillatory; this is representative of the layered packing of CCl_4 at the CCl_4−H_2O interface and has been studied in detail elsewhere.[26]

Figure 1b shows the density profiles of hydrogen bond acceptors and water monomers. Similar to straddling water molecules, hydrogen bond acceptors also possess peak populations at the interface. The hydrogen bond acceptor population

(29) Case, D. A., et al. *AMBER 7*; University of California: San Francisco, 2002.
(30) Morita, A.; Hynes, J. T. *Chem. Phys.* **2000**, *258*, 371.
(31) Walker, D. S.; Hore, D. K.; Richmond, G. L. *J. Phys. Chem. B* **2006**, *110*, 20451.
(32) Strutwolf, J.; Barker, A. L.; Gonsalves, M.; Caruana, D. J.; Unwin, P. R.; Williams, D. E.; Webster, J. R. P. *J. Electroanal. Chem.* **2000**, *483*, 163.

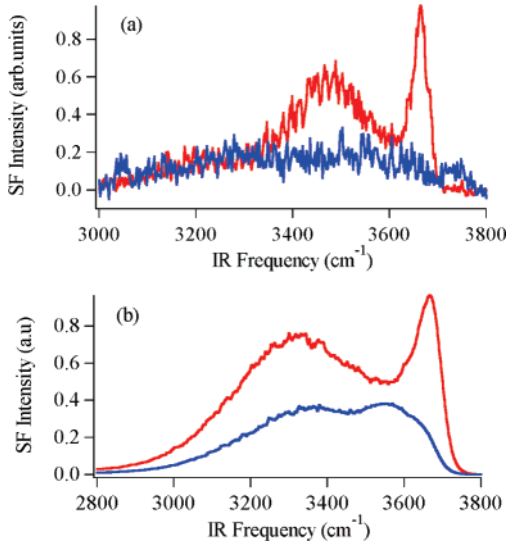

Figure 2. (a) Experimental and (b) computational VSF spectral intensities of the CCl_4-H_2O (red) and DCE$-H_2O$ (blue) interfaces in SSP polarization. Resolution (bin size) for computational spectrum is 1 cm^{-1}.

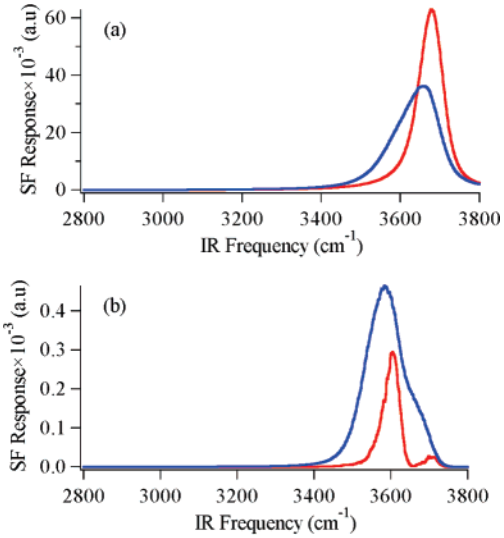

Figure 3. Computational VSF spectral intensities of (a) the free OH mode from straddling water molecules and (b) hydrogen bond acceptors at the CCl_4-H_2O (red) and DCE$-H_2O$ (blue) interfaces in SSP polarization. The spectral response from hydrogen bond acceptors at the CCl_4-H_2O interface has been scaled by 10× to fit the graph. Resolution (bin size) for computational spectra is 1 cm^{-1}.

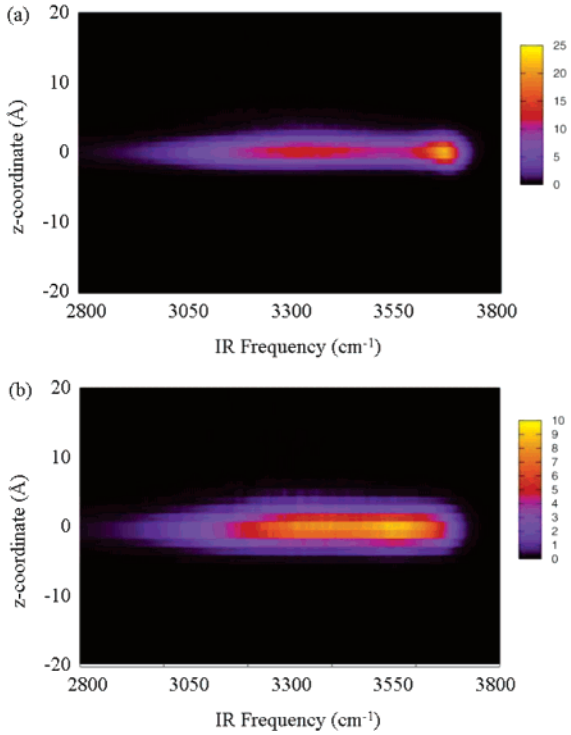

Figure 4. Computational VSF spectral profiles of water at the (a) CCl_4-H_2O and (b) DCE$-H_2O$ interfaces as functions of frequency (vertical axis) and interfacial depth (horizontal axis) in SSP polarization. Resolution (bin size) for each graph is 1 Å and 1 cm^{-1}.

is significantly greater in the DCE$-H_2O$ system compared to the CCl_4-H_2O system and possesses a peak population that extends deeper into the DCE phase than the CCl_4 phase. Similar to the density profiles of straddling water molecules, the density profile of water monomers in the CCl_4-H_2O system also possesses peak population at the interface. However, the density profile of water monomers at the DCE$-H_2O$ interface persists in population throughout the organic phase. This observation, in addition to that of an increased hydrogen bond acceptor population, is consistent with the increased solubility of water in DCE compared to CCl_4.

Figure 2a and 2b show respectively the experimental and computational VSF spectral intensities of water at the CCl_4-H_2O and DCE$-H_2O$ interfaces in SSP polarization. The computational CCl_4-H_2O spectrum reasonably reproduces the spectral features seen in the experimental result, and the computational DCE$-H_2O$ spectrum adequately demonstrates the loss of structure and intensity observed experimentally. A detailed computational deconvolution of these spectra has been reported elsewhere.[28]

Figure 3a and 3b show computational VSF spectral intensities of the free OH mode (from straddling water molecules) and hydrogen bond acceptors, respectively, at the CCl_4-H_2O and DCE$-H_2O$ interfaces in SSP polarization. Figure 3a shows the free OH mode at the CCl_4-H_2O interface is determined to possess a peak value of 3670 cm^{-1}, in excellent agreement with experimental measurements.[10] The free OH mode at the DCE$-H_2O$ interface, though not readily apparent from Figure 2a and 2b, is shown to be the largest spectral contributor to the total DCE$-H_2O$ spectrum in SSP polarization.[28]

Figure 3b shows that the computational VSF spectral intensity of hydrogen bond acceptors at the CCl_4-H_2O interface, though scaled by a factor of 10, is still small compared to the spectral response of hydrogen bond acceptors at the DCE$-H_2O$ interface. For hydrogen bond acceptors at the CCl_4-H_2O interface, two clear peaks are observed that correspond to symmetric (3605 cm^{-1}) and antisymmetric (3710 cm^{-1}) OH stretch modes, in good agreement with past experimental measurements.[10] The increased VSF spectral intensity of hydrogen bond acceptors at the DCE$-H_2O$ interface is shown to cause interference effects with the free OH mode (Figure 3a) that result in the loss of a distinct free OH peak at the DCE$-H_2O$ interface (see Figure 2a and 2b).[28]

Figure 4a and 4b show computational VSF spectral profiles of water at these liquid−liquid systems as functions of both frequency and interfacial depth. For these graphs, the horizontal axis represents the frequency and the vertical axis represents the *z*-coordinate. As is the case with Figures 1a and 1b, the

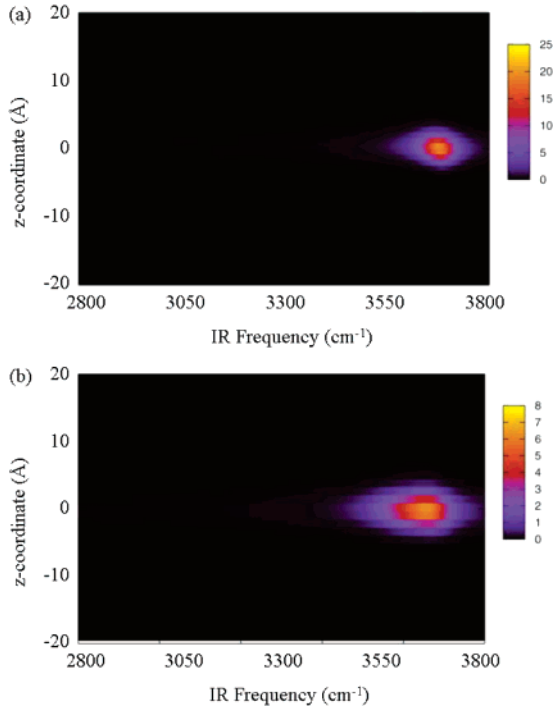

Figure 5. Computational VSF spectral profiles of the free OH mode at the (a) CCl_4-H_2O and (b) $DCE-H_2O$ interfaces in SSP polarization. Resolution (bin size) for each graph is 1 Å and 1 cm^{-1}.

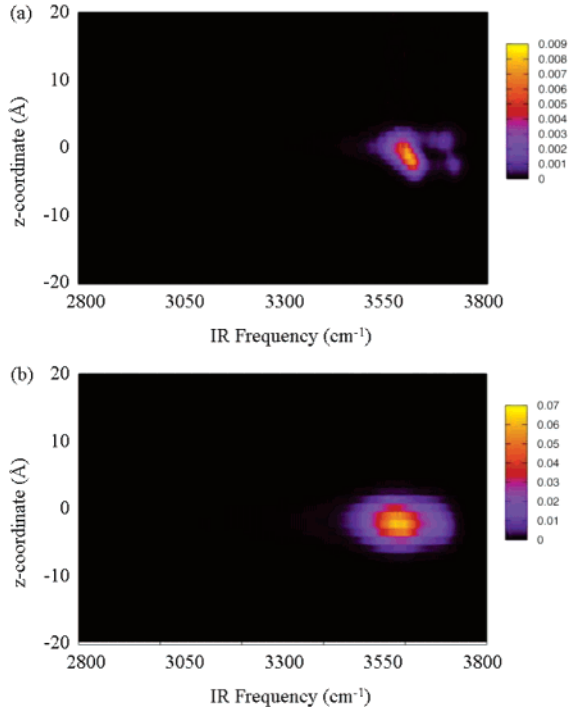

Figure 6. Computational VSF spectral profiles of hydrogen bond acceptors at the (a) CCl_4-H_2O and (b) $DCE-H_2O$ interfaces in SSP polarization. Resolution (bin size) for each graph is 1 Å and 1 cm^{-1}.

density region above 0 Å represents the water phase, while the density region below 0 Å represents the organic phase. Figure 4a shows the VSF spectral profile of water at the CCl_4-H_2O interface as a function of interfacial depth. This profile identifies two key features: the peak intensity of the free OH stretch mode at high frequencies, and a relatively thin region of spectral intensity as a function of interfacial depth observed at lower frequencies. Figure 4b shows the VSF spectral profile of water at the $DCE-H_2O$ interface as a function of interfacial depth. Relative to the CCl_4-H_2O depth profile, the VSF response from water at the $DCE-H_2O$ interface is more diffuse, indicative of a broader region of oriented water molecules at this interface relative to the CCl_4-H_2O interface. Particularly interesting is that, unlike the CCl_4-H_2O interface, the free OH peak located at high frequencies is not distinguishable at the $DCE-H_2O$ interface. These graphs combine the information that can be extracted from VSF spectral intensities (Figure 2b) and density profiles (Figure 1a) to demonstrate visually the increased interfacial thickness at the $DCE-H_2O$ interface relative to the CCl_4-H_2O interface. Further analysis to follow will show the depth profiles of different types of water species that interact directly with the organic phase, information that can be quite elusive with the more traditional analytical approaches featured in Figures 1 and 2.

Figure 5a and 5b show computational VSF spectral profiles of the free OH mode at the CCl_4-H_2O and $DCE-H_2O$ interfaces, respectively. Water molecules that straddle the interface (with one OH bond extended into the water phase and the other "free" OH bond extended into the organic phase) are responsible for producing this type of OH stretch mode. The OH bond extended into the water phase is hydrogen bonded to an adjacent water molecule as a proton donor. The oxygen atom of straddling water molecules can also hydrogen bond to adjacent water molecules as a single or double proton acceptor. Although these straddling water molecules are shown to exist throughout the entire water region based on their criterion for hydrogen bonding (see Figure 1a), Figure 5a and 5b show that the spectral response of the free OH mode only resides at the interface. This is due to the isotropic nature of bulk water and the anisotropic nature of the water surface under the dipole approximation. Unlike the CCl_4-H_2O VSF response (experimental or computational), the $DCE-H_2O$ VSF response (experimental or computational) displays no distinct spectral contribution from the free OH mode even though these calculations indicate it is present (see also Figure 3a). Compared to the spectral profile of the free OH mode at the CCl_4-H_2O interface (Figure 5a), the spectral profile of the free OH mode at the $DCE-H_2O$ interface (Figure 5b) is broader in both frequency and depth, indicative of a broader range of interactions between DCE and H_2O at the interface. We attribute the asymmetric tail of spectral intensity found at lower frequencies (Figure 5b and 3a) to stronger interactions between the free OH mode and the DCE phase relative to those between the free OH mode and the CCl_4 phase. The spectral characterization of the free OH mode has been identified from a computational deconvolution of the VSF spectral intensity measured at the $DCE-H_2O$ interface.[28] In that work, the free OH mode was found to be the single largest contributor at the $DCE-H_2O$ interface, but spectral interferences with hydrogen bond acceptors resulted in its absence from the total $DCE-H_2O$ spectrum. These studies provide further insight into the interfacial depth of straddling water molecules by spatially isolating the region of the interface where they exhibit net molecular orientation.

Figure 6a and 6b show computational VSF spectral profiles of hydrogen bond acceptors at the CCl_4-H_2O and $DCE-H_2O$ interfaces, respectively. Hydrogen bond acceptors interact with adjacent water molecules only through one or two intermolecular hydrogen bonds to their oxygen atoms. Figure 6a shows

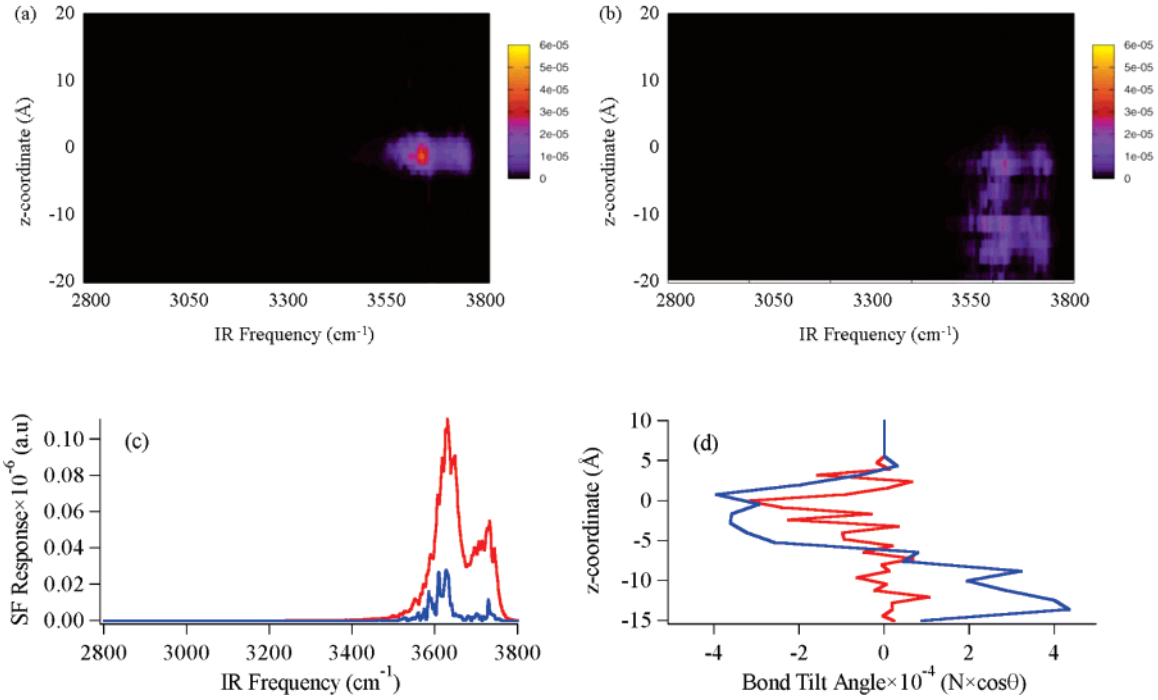

Figure 7. (a) Computational VSF spectral profile of water monomers at the CCl_4-H_2O interface. (b) Computational VSF spectral profile of water monomers at the DCE$-H_2O$ interface. (c) Computational VSF spectral intensities of water monomers at the CCl_4-H_2O (red) and DCE$-H_2O$ (blue) interfaces. (d) Tilt angle distributions of OH bonds from water monomers at the CCl_4-H_2O (red) and DCE$-H_2O$ (blue) interfaces. Resolution (bin size) for each graph is 1 Å and/or 1 cm^{-1}.

interesting new information about such hydrogen bond acceptors at the CCl_4-H_2O interface. The OH oscillators of hydrogen bond acceptors exist in similar (organic) environments, resulting in clear symmetric and antisymmetric OH stretch modes (see also Figure 3b). These OH stretch modes have been identified experimentally.[10] For a given value of interfacial depth in Figure 6a, the symmetric OH stretch mode is observed as part of the more intense lower frequency peak, while the antisymmetric OH stretch mode is observed as an isolated, lower intensity peak at higher frequencies. Progressing along the *z*-coordinate from the water phase (above 0 Å) toward the CCl_4 phase (below 0 Å), both the symmetric and antisymmetric peaks shift toward slightly higher frequencies. This difference in spectral location as a function of interfacial depth is likely caused by separate spectral contributions between water molecules that possess only one acceptor bond compared to those that possess two acceptor bonds, with molecules possessing two acceptor bonds located closer to the water phase. Figure 6b shows a broad, somewhat featureless spectral profile for hydrogen bond acceptors at the DCE$-H_2O$ interface that corresponds primarily to its symmetric OH stretch mode. The asymmetric tail of spectral intensity found at higher frequencies is attributed to the antisymmetric OH stretch mode of hydrogen bond acceptors, whose peak has more overlap with the symmetric OH stretch mode than that observed at the CCl_4-H_2O interface. Spectral deconvolution of the computational VSF spectral intensities reveals this mode to be approximately 1 order of magnitude larger at the DCE$-H_2O$ interface compared to the CCl_4-H_2O interface (see also Figure 3b).[28]

Figure 7a shows the computational VSF spectral profile of water monomers (non-hydrogen-bonded water molecules) at the CCl_4-H_2O interface. As is predicted based upon the localization of its density profile (see Figure 1b), the spectral profile of water monomers is localized around the interfacial region. Similar to hydrogen bond acceptors at this interface (see Figure 3b), water monomers exhibit lower and higher vibrational frequencies corresponding to symmetric and antisymmetric OH stretch modes, respectively. Figure 7b shows the computational VSF spectral profile of water monomers at the DCE$-H_2O$ interface. The spectral profile of water monomers in this system also follows its density profile in Figure 1b. However, it is somewhat surprising that, deep into the DCE phase, water monomers still appear to be *oriented*. The spectral profile from water monomers at the DCE$-H_2O$ interface is the only spectral profile that produces a detectable spectral response from any species of water beyond the immediate interfacial region. (This profile is 5 orders of magnitude smaller than that of the entire DCE$-H_2O$ spectral profile shown in Figure 4b; therefore it does not significantly contribute to that result.) The observation of oriented water monomers deeply immersed within the DCE phase would be very difficult to elucidate from Figure 7c, which shows computational VSF spectral intensities of water monomers at the DCE$-H_2O$ and CCl_4-H_2O interfaces. Figure 7c shows that the VSF spectral intensity of water monomers at the DCE$-H_2O$ interface is actually *smaller* than that of the CCl_4-H_2O interface.

In general, VSF responses from water molecules are dependent upon both population and net orientation. Figure 1b shows that water monomers at the DCE$-H_2O$ interface have greater populations than water monomers at the CCl_4-H_2O interface. To address the orientation dependence of water monomers within these systems, Figure 7d shows tilt angle distributions of OH bonds from water monomers at the CCl_4-H_2O and DCE$-H_2O$ interfaces. Positive tilt angle values represent OH bonds oriented with the hydrogen atom directed toward the organic phase, while negative tilt angle values represent OH bonds oriented with the hydrogen atom directed toward the water phase. 30 Å of bulk water were excluded in the data collection,

which correlates to *z*-coordinate values greater than 5 Å. Figure 7d reveals that water monomers at the CCl_4-H_2O interface generally point their OH bonds toward the water phase, while those at the DCE$-H_2O$ interface are sensitive to their degree of immersion within the organic phase: Water monomers closest to the DCE$-H_2O$ interface direct their OH bonds toward water, while those further away direct their OH bonds toward DCE. The small VSF spectral intensity of water monomers at the DCE$-H_2O$ interface (Figure 7c) is attributed to destructive interference effects caused by two separate spatial regions of oppositely oriented water monomers. This differs significantly from destructive spectral interferences that are typically observed from (nearly) isotropic distributions of molecules, but both types of molecular environment could produce the same spectral response when plotted as a function of frequency alone. While other types of water molecules experience a broad range of interactions at the DCE$-H_2O$ interface compared to the CCl_4-H_2O interface, water monomers at the DCE$-H_2O$ interface are expected to experience the broadest range of interactions of all types of water molecules due to their degree of penetration into the DCE phase.

Conclusions

Molecular dynamics simulations have been applied to produce vibrational sum frequency (VSF) spectral profiles of water at the CCl_4-H_2O and DCE$-H_2O$ interfaces. These spectral profiles provide new insights into the presence and interfacial depth of water molecules that interact directly with the organic phase. Unlike density profiles that describe interfacial thickness by changes in molecular population, spectral profiles describe interfacial thickness by changes in molecular orientation, thus revealing the anisotropic nature of the liquid surface. In addition, this computational approach enables direct comparison with VSF measurements performed experimentally, and in doing so a reliable description of interfacial water structure is provided. The combined experimental and computational approach allows for a better understanding of the interfacial region and the species of water that are present at different depths, information that cannot be obtained by the VSF experimental measurements alone.

The results show clear differences in the structure and orientation of liquid water in contact with a nonpolar organic liquid (CCl_4) versus a slightly polar organic liquid (DCE). The spectral profiles show that the CCl_4-H_2O interface has a narrow interfacial region of oriented water molecules, while the DCE$-H_2O$ interface is measurably broader. The increased width of the DCE$-H_2O$ interface is consistent with results obtainable from density profiles. In addition, these spectral profiles show that even though the DCE$-H_2O$ interface is broader and seemingly more diffuse, water molecules present throughout the interfacial region show a high degree of net orientation. In the deconvolution of the spectral profiles, emphasis is placed upon those water molecules that contain OH stretch modes interacting directly with the organic phase: the free OH mode from straddling water molecules, hydrogen bond acceptors, and water monomers. The spectral profiles of these types of molecules show how two liquid−liquid interfacial regions differ in the extent of spectral and interfacial broadening associated with the free OH mode, the spatial resolution of hydrogen bond acceptors that possess one or two intermolecular hydrogen bonds, and the presence of oriented water monomers that are found to deeply penetrate into the DCE phase.

This computational approach combines two standard interfacial treatments to create a new visual tool for understanding interfacial structure and environment. The comparison of the calculations with experiments adds more credibility to the models used in the simulation, and the combined approach provides information about interfacial depth and bonding not easily accessible by VSF experiments alone. Whereas the results described in this work are shown to be useful in the comparative study of two different liquid−liquid systems, this approach is readily adaptable to perturbations made onto individual systems. An important example includes understanding water structure in the double layer region created by surfaces in the presence of interfacial ions and surfactants. Such studies at the vapor−water and oil−water interfaces are currently in progress in this laboratory.

Acknowledgment. The authors thank the National Science Foundation (CHE 0652531) and the Basic Energy Sciences of the Department of Energy (DEFG02-96ER45557) for supporting this study.

Supporting Information Available: Complete citation for ref 29. This material is available free of charge via the Internet at http://pubs.acs.org.

JA071740B